Cell Reports

Touch Receptors Undergo Rapid Remodeling in Healthy Skin

Graphical Abstract

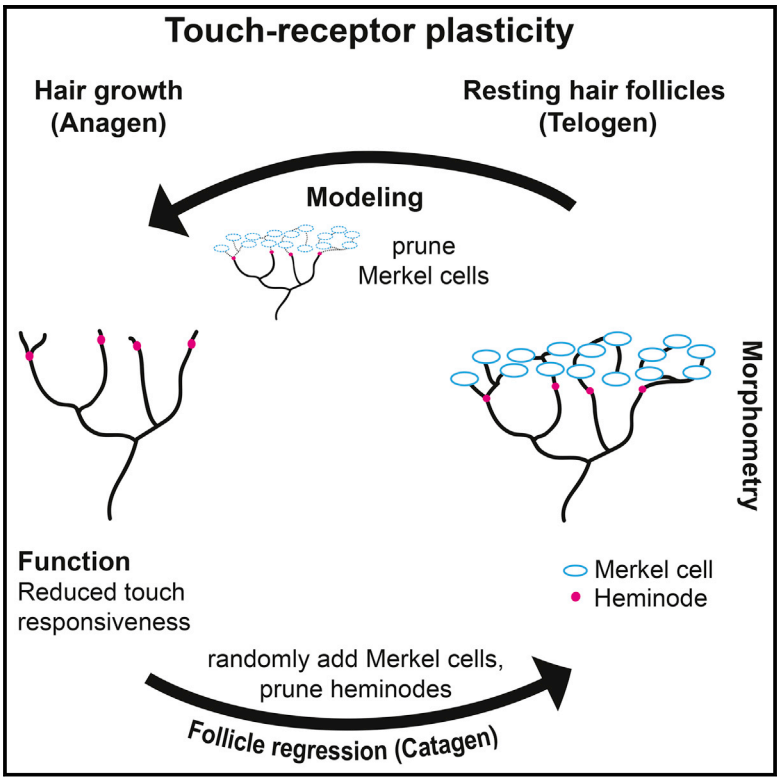

Highlights

- Tactile sensory afferents are highly plastic during hair growth in mice
- Merkel cells are reduced and neuronal arbors are simplified in anagen touch domes
- Tactile behavior and electrophysiology show decreased reliability during hair growth
- Simulations reveal simple rules that explain Merkel cell-neurite complex remodeling

Authors

Kara L. Marshall, Rachel C. Clary, Yoshichika Baba, Rachel L. Orlowsky, Gregory J. Gerling, Ellen A. Lumpkin

Correspondence

eal2166@columbia.edu

In Brief

Sensory neurons must maintain peripheral innervation patterns during turnover of target epithelia. Marshall et al. report a reduction in mechanosensory Merkel cells and simplification of tactile afferent endings in mouse skin during hair renewal, with an accompanying impairment in tactile responsiveness. This reveals remarkable peripheral neuron plasticity in healthy skin.

Marshall et al., 2016, Cell Reports *17*, 1719–1727
November 8, 2016
http://dx.doi.org/10.1016/j.celrep.2016.10.034

CellPress

Cell Reports
Report

Touch Receptors Undergo Rapid Remodeling in Healthy Skin

Kara L. Marshall,[1,2,7] Rachel C. Clary,[1,3,7] Yoshichika Baba,[1] Rachel L. Orlowsky,[4,5] Gregory J. Gerling,[4,5] and Ellen A. Lumpkin[1,2,3,6,8,*]

[1]Department of Physiology and Cellular Biophysics, Columbia University, New York, NY 10032, USA
[2]Integrated Training Program in Cellular, Molecular and Biomedical Sciences, Columbia University, New York, NY 10032, USA
[3]Neurobiology and Behavior Training Program, Columbia University, New York, NY 10032, USA
[4]Department of Systems and Information Engineering, University of Virginia, Charlottesville, VA 22904, USA
[5]Department of Biomedical Engineering, University of Virginia, Charlottesville, VA 22904, USA
[6]Department of Dermatology, Columbia University, New York, NY 10032, USA
[7]Co-first author
[8]Lead Contact
*Correspondence: eal2166@columbia.edu
http://dx.doi.org/10.1016/j.celrep.2016.10.034

SUMMARY

Sensory tissues exposed to the environment, such as skin, olfactory epithelia, and taste buds, continuously renew; therefore, peripheral neurons must have mechanisms to maintain appropriate innervation patterns. Although somatosensory neurons regenerate after injury, little is known about how these neurons cope with normal target organ changes. To elucidate neuronal plasticity in healthy skin, we analyzed the structure of Merkel-cell afferents, which are gentle touch receptors, during skin remodeling that accompanies mouse hair-follicle regeneration. The number of Merkel cells is reduced by 90% and axonal arbors are simplified during active hair growth. These structures rebound within just days. Computational modeling predicts that Merkel-cell changes are probabilistic, but myelinated branch stability depends on Merkel-cell inputs. Electrophysiology and behavior demonstrate that tactile responsiveness is less reliable during active growth than in resting skin. These results reveal that somatosensory neurons display structural plasticity at the cost of impairment in the reliability of encoding gentle touch.

INTRODUCTION

Sensory stimuli are encoded by the peripheral nervous system, which displays a remarkable ability to regenerate (Chen et al., 2007). Several sensory tissues continuously renew, which is proposed to play a role in maintenance and sensory optimization (Feng et al., 2014; Mouret et al., 2009). In skin, tactile afferents innervate discrete sensory structures, such as touch domes or hair follicles, which regenerate throughout an animal's lifetime (Plikus and Chuong, 2008; Schneider et al., 2009). Although the structural plasticity of somatosensory neurons that innervate skin has been studied in the context of injury and disease, little is known about their plasticity in healthy tissue (Cheng et al., 2010; Rajan et al., 2003) Thus, hair growth provides an opportunity to study how somatosensory afferents respond to normal target-organ remodeling.

Mouse hair growth is synchronized, resulting in periods of massive cellular turnover and skin structural changes (Müller-Röver et al., 2001). Two reports indicate that innervation density increases during hair growth (Botchkarev et al., 1997; Peters et al., 2001). Similarly, Merkel cells, which are epidermal components of gentle touch receptors, have been reported to be more abundant during follicle growth (Moll et al., 1996; Nakafusa et al., 2006). These studies suggest that cutaneous neurons and Merkel cells engage plasticity mechanisms during hair-follicle regeneration; however, the dynamics and physiological consequences of neuronal plasticity in touch receptors are unknown.

To address this gap, we analyzed the structure and function of Merkel-cell afferents over the mouse hair cycle. Merkel cells and their afferents produce slowly adapting (SA) type I (SAI) responses, which encode pressure and object features (Johnson et al., 2000; Maksimovic et al., 2014; Woo et al., 2014). We report that Merkel-cell afferents undergo rapid remodeling during healthy skin renewal, which is accompanied by transient impairment in gentle-touch responses.

RESULTS

The Hair Cycle Stimulates Touch-Receptor Remodeling

To assess neuronal plasticity in healthy skin, we analyzed peripheral end organs of Merkel-cell afferents in the mouse hindlimb throughout complete hair cycles, which are governed by molecular crosstalk between follicle stem cells and neighboring cells (Alonso and Fuchs, 2006; Jahoda and Christiano, 2011; Plikus and Chuong, 2008). The hair cycle comprises three stages: telogen, a resting phase when stem cells are quiescent; anagen, the

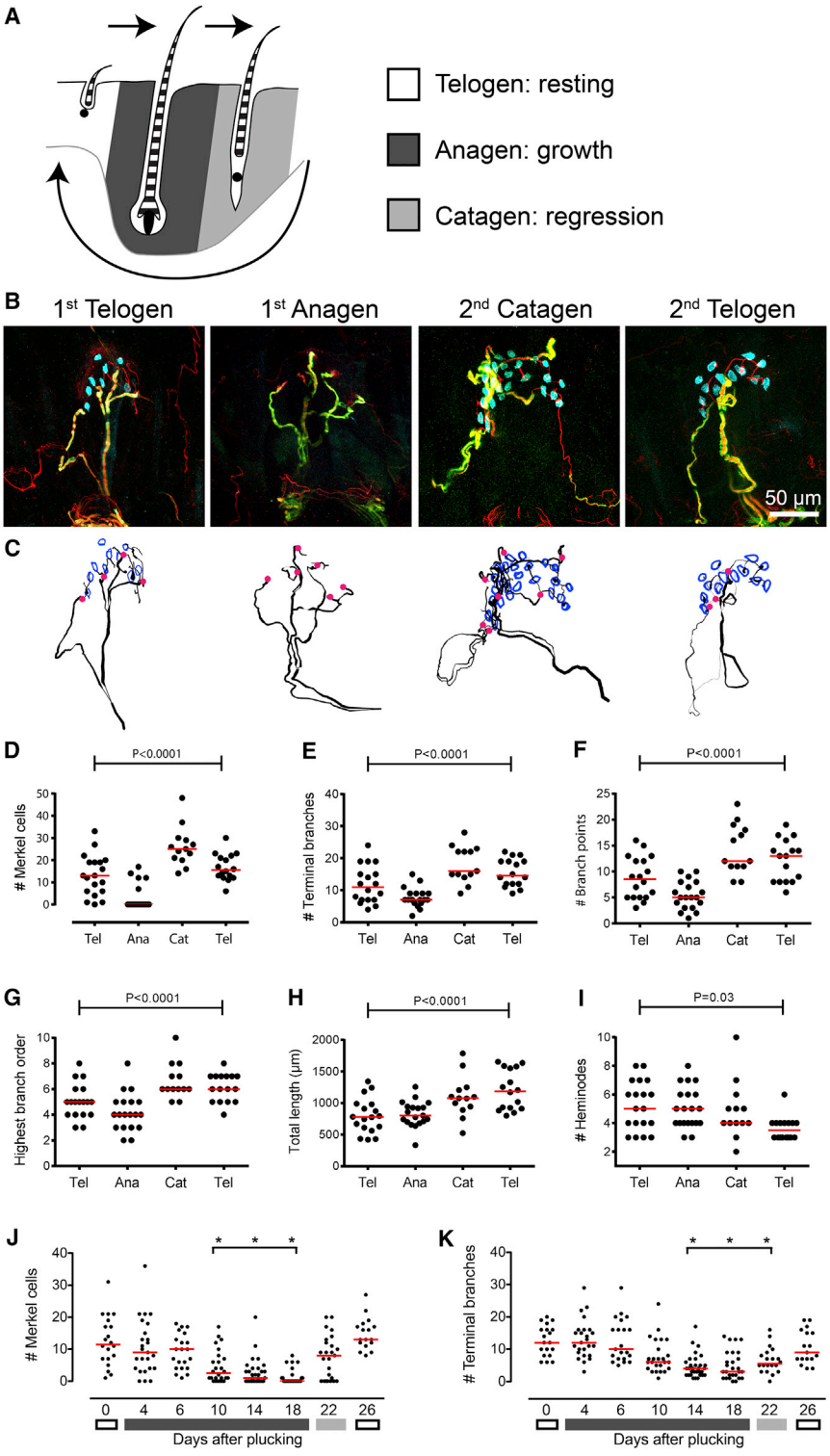

Figure 1. Touch Receptors Show Plasticity during the Hair Cycle

(A) Diagram shows the mouse hair cycle.

(B) Representative axial projections show touch domes in *Atoh1/nGFP* mouse hindlimb during a spontaneous hair cycle: first telogen (P28), late anagen (stages IV–VI; P39), catagen (stages III–XIII; P40), and second telogen (P66). K8, cyan; NFH, red; MBP, green. Scale applies to all panels.

(C) Neurolucida tracing of projections from (B). Merkel cells are outlined in blue. Magenta dots mark heminodes.

(D–I) Quantitative morphometry showing Merkel cell number (D), number of terminal branches (E), number of branch points (F), highest branching order (G), total afferent length (H), and number of heminodes, identified as endpoints of MBP staining (I). The p values are results from one-way ANOVAs (n = 13–19 touch domes from three to four animals per group).

(J and K) Quantification of Merkel cells (J) and terminal neurites in NFH+ afferents during an induced hair cycle (K; n = 17–31 touch domes from three to four mice per group; $p < 0.0001$ for both measures, one-way ANOVA). Asterisks denote groups that significantly differed from day 0 (P68–P70) by Tukey's post hoc comparisons. Grayscale bars indicate hair-cycle stage as in (A). For (D)–(K), each point represents a single touch dome and red lines denote median values. See also Movies S1, S2, S3, and S4 for 3D reconstructions and Figures S1–S3.

growth phase when follicles nearly triple in length; and catagen, a regression phase (Fuchs, 2009; Schneider et al., 2009). In pigmented mice, skin color darkens during anagen, which facilitates hair-cycle staging (Figure 1A; Müller-Röver et al., 2001).

Whole-mount immunohistochemistry was used to visualize touch receptor endings in their entirety (Figure 1B). Specimens were stained for markers of mature Merkel cells (Keratin 8 [K8]; Kim and Holbrook, 1995), myelinated afferents (Neurofilament H [NFH]), and myelin (myelin basic protein [MBP]; Lesniak et al., 2014). Merkel-cell afferents were identified based on morphology and juxtaposition to guard hair follicles (Iggo and Muir, 1969), which were recognized by their NFH-positive lanceolate endings (Bai et al., 2015; Li et al., 2011). Merkel-cell afferents, which branch to contact Merkel cells, can be distinguished from other NFH-positive afferents based on two additional anatomical features. First, their myelin endpoints lie just beneath the epidermal-dermal border (Lesniak et al., 2014). Second, their unmyelinated neurites penetrate the epidermis. In telogen, 94% of afferents that met these criteria innervated Merkel cells (n = 97; Lesniak et al., 2014).

We first asked whether tactile afferents undergo plasticity during the spontaneous hair cycle (post-natal day [P]28–P70 in

hindlimb skin; Figure S1). Three-dimensional (3D) reconstructions were used to trace Merkel-cell afferents from the dermal nerve plexus to the epidermis (Figure 1C; Movies S1, S2, S3, and S4). Morphometric quantification revealed that Merkel cells and terminal neurites were unexpectedly dynamic over the hair cycle (Figures 1D and 1E). Surprisingly, two-thirds of touch domes lacked K8-positive Merkel cells in late anagen. Anagen afferents also displayed few terminal branches (Figure 1E), and, in many cases, they lacked branching neurites that normally extend from myelin endpoints. In these arbors, NFH immunoreactivity was often diffuse, resembling swollen neuronal terminals observed during Wallerian degeneration (Figure S2; Dubový and Aldskogius, 1996; Hsieh et al., 2000). Merkel cells and terminal branches rebounded in catagen. These results reveal that Merkel-cell afferents are capable of dramatic structural plasticity during the spontaneous hair cycle.

To assess the extent of neuronal remodeling, we next analyzed arbor complexity. The number of branch points and highest branch order, a measure of nested branching, fluctuated in a pattern that mirrored Merkel-cell numbers (Figures 1F and 1G). Unexpectedly, branching parameters only correlated with Merkel-cell number in catagen (Figure S3; $p = 0.002–0.01$, Pearson's correlation). Total afferent length progressively increased over the hair cycle (Figure 1H), whereas number of heminodes, which are sites of spike initiation at myelin endpoints (Figure 1I; Lesniak et al., 2014), decreased from anagen to second telogen (Figure 1I). Together these data suggest that unmyelinated branches become more complex as Merkel-cell numbers rebound whereas myelinated branches refine over the hair cycle.

To analyze temporal dynamics of end-organ remodeling, we used a controlled model of hair cycling. Anagen was induced by plucking hair from 2-cm^2 patches of hindlimb skin (Plikus et al., 2008), and specimens were analyzed at 2- to 4-day intervals over a complete cycle (Figure S1; Plikus et al., 2008). The number of Merkel cells per touch dome progressively decreased from telogen (day 0) through late anagen (days 10–18), with 63% of touch domes lacking Merkel cells at day 18 (Figure 1J). Remaining Merkel-cell clusters were also smaller in late anagen (day 18: 3.6 ± 2.7 Merkel cells, mean $\pm$ SD, $n = 10$) compared with telogen (day 0: 12.6 ± 7.7, $n = 20$; $p = 0.001$, Student's two-tailed t test), resulting in a 90% reduction of Merkel cells overall. Merkel cells recovered in catagen (day 22; Figure 1J), only 4 days after the nadir. Terminal neurites decreased in tandem with Merkel cells through anagen, and then arbors returned to resting stage structures within 8 days (day 26; Figure 1K). Thus, Merkel cell-neurite complexes show rapid structural changes during hair growth.

To determine whether remodeling is a general feature of touch-dome afferents, we reconstructed touch domes at a second body site (Figure 2A). Back skin was chosen to match previous studies (Moll et al., 1996; Nakafusa et al., 2006). As in hindlimb skin, back skin afferents had fewest Merkel cells and terminal branches in late anagen, with 52% of anagen touch domes lacking K8-positive Merkel cells ($n = 23$; Figures 2B and 2C). We also tested alternate Merkel-cell markers in anagen, catagen, and telogen. We found that 77% of K8-positive Merkel cells expressed the early marker Atoh1-GFP ($n = 391$ from five mice; Figure 2D; Wright et al., 2015). VGLUT2 immunoreactivity, which is found in mature Merkel cells and touch dome afferents (Haeberle et al., 2004), co-localized with K8 in 96% of Merkel cells ($n = 489$ from five mice; Figure 2E). Importantly, touch domes that lacked K8-positive cells showed no Atoh1-GFP expression (Figure 2F; $n = 19$ touch domes) or VGLUT2-positive epidermal cells (Figure 2G; $n = 11$ touch domes). Thus, neither regional differences in end-organ plasticity nor selective loss of K8 explains the changes in Merkel-cell numbers we observed.

We wondered whether neuronal sprouting outside of touch domes might explain the abundance of anagen afferents lacking Merkel cells. Indeed, the density of myelinated afferents terminating near the epidermis increased in anagen compared with catagen (Figure S4). Thus, newly sprouted myelinated branches could account for some low-complexity arbors in late anagen; however, sprouting cannot explain the progressive decline in Merkel cells and neurites between telogen and late anagen (Figure 1J).

To identify principles that specify how arbors change over the hair cycle, we built a computational model to evaluate policies of Merkel-cell and heminode dynamics (Figure 3). Thirty end organs were auto-generated by clustering Merkel cells at heminodes, whose numbers were probabilistically drawn from first-telogen distributions (Figures 1D and 1I). Each end organ then went through a complete hair cycle, with iterations of remodeling following four policies: (1) the probability of losing a Merkel cell from a cluster is proportional to cluster size, (2) the probability of adding a Merkel cell is random across heminodes, (3) myelinated branches refine to achieve a range of three to four heminodes, and (4) heminodes that lack Merkel cells are most likely to be pruned (Figure 3A). These simple rules produced distributions of Merkel cells (Figure 3B) and heminodes (Figure 3C) in anagen, catagen, and telogen that agreed with experimental observations (compare with Figures 1D and 1I). Thus, we propose that Merkel-cell loss and addition are probabilistic among heminodes but that the stability of heminodes, and thus myelinated branches, depends on Merkel-cell inputs.

Touch-Receptor Reliability Is Compromised during Skin Remodeling

Next, we assessed the functional consequences of afferent plasticity. To determine whether force-sensing machinery was intact in anagen, we assessed the expression of a transgenic Piezo2-GFP reporter (Figure S4; Woo et al., 2014). Piezo2, a mechanosensitive ion channel critical for gentle touch (Ranade et al., 2014), was observed in all touch-dome afferents, including those that lacked terminal neurites, which suggests that anagen afferents can transduce mechanical stimuli.

To measure touch-evoked firing of Merkel-cell afferents over the spontaneous hair cycle, we used an ex vivo skin-nerve preparation to record from Aβ low-threshold mechanoreceptors (LTMRs) whose end organs were visualized by FM1-43 labeling (Maksimovic et al., 2014; Wellnitz et al., 2010). Merkel-cell afferents produce SAI responses, which are characterized by receptive fields limited to touch domes, high-frequency dynamic firing, low-frequency sustained firing with irregular interspike intervals, and a lack of response to guard-hair movement (Iggo and Muir, 1969). In an unbiased survey of Aβ LTMRs, we observed canonical SAI responses in 5% (1/20) of anagen afferents compared

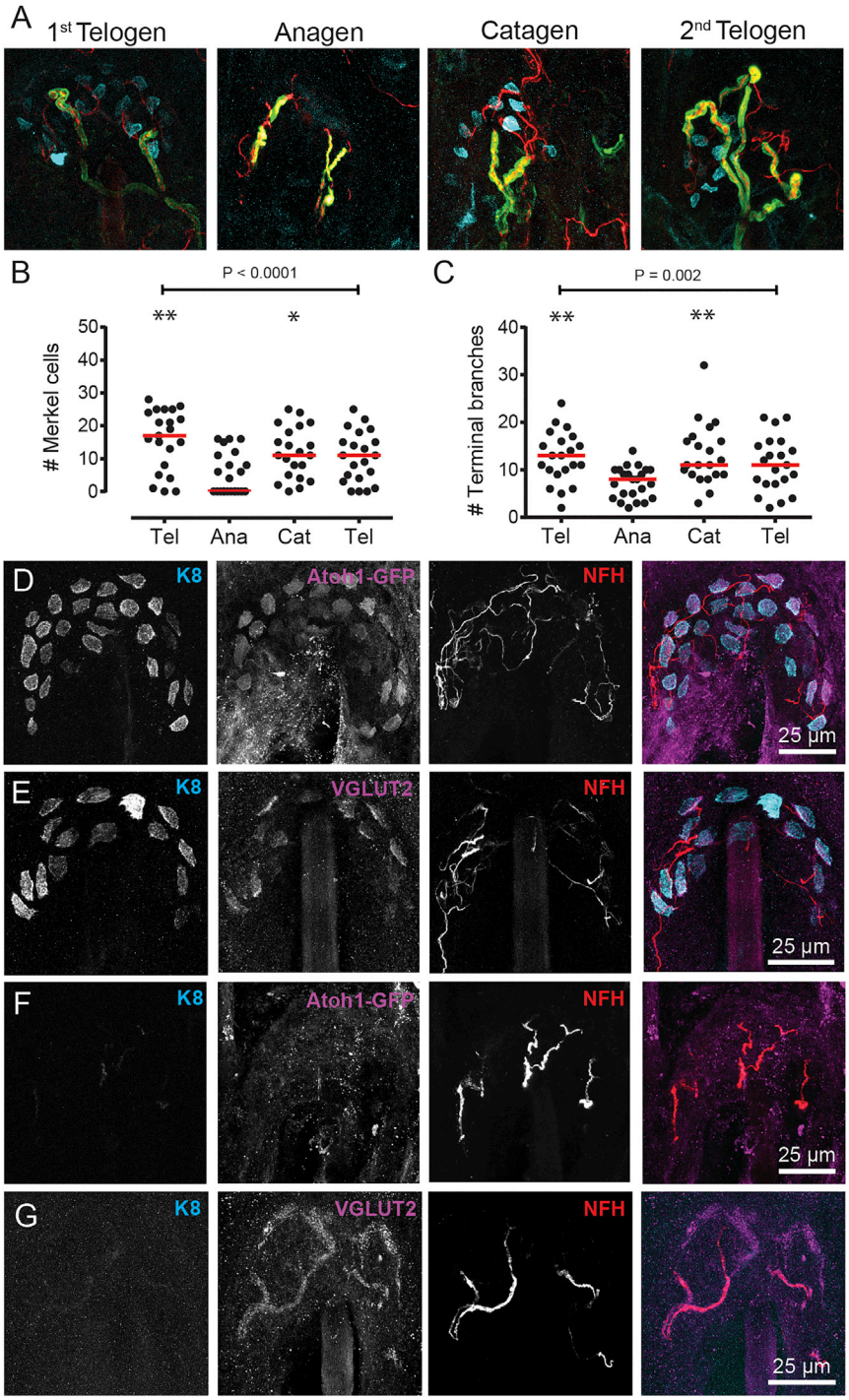

Figure 2. Afferent Remodeling Is Observed across Skin Regions and Merkel-Cell Markers

(A) Axial projections show touch domes in back skin during a spontaneous hair cycle: first telogen (P23), anagen (stages IV–VI; P35), catagen (stages I–II; P44), and second telogen (P70). K8, cyan; NFH, red; MBP, green.

(B and C) Quantitative morphometry of Merkel cells (B) and terminal branches (C). The p values are results from one-way ANOVAs (n = 21–23 touch domes from two to three animals per group). Asterisks indicate groups significantly different from anagen based on Tukey's post hoc comparisons (*p = 0.03 and **p < 0.003). Red lines, medians.

(D–G) Axial projections show touch domes containing (D and E) or lacking (F and G) K8+ Merkel cells stained with antibodies against GFP (*Atoh1*$^{A1GFP/A1GFP}$ mice; D and F) or VGLUT2 (E and G) in hindlimb skin during a spontaneous hair cycle. K8, cyan; NFH, red; Atoh1-GFP or VGLUT2, magenta. Images are representative of 43–46 touch domes from five mice per marker. See also Figure S4.

with 26% (5/19) in telogen (Table S1). These results indicate that SAI responses occur less frequently in anagen, when Merkel-cell afferents show reduced arbor complexity.

We next used targeted recordings to analyze SAI responses in spontaneous anagen (Figures 4A and 4D), catagen (Figures 4B and 4E), and telogen (Figures 4C and 4F). The sensitivity of each afferent's response was estimated by fitting force-firing rate curves during dynamic and static stimulus phases with Boltzmann relations (Figures 4G–4I). Boltzmann slope was used as a measure of mechanical sensitivity, with lower values signifying steeper curves and, thus, higher sensitivity. Mechanical set-points were estimated from the mid-points of force-firing curves (F_{50}), as well as force threshold, defined as the lowest stimulus amplitude that elicited reliable firing. Maximal firing rates did not differ across hair-cycle stages (Figure 4J).

When stimulus-response parameters of Merkel cell afferents were compared, we found that median values were indistinguishable across hair-cycle stages ($p > 0.05$, Kruskal-Wallis tests); however, fit parameters followed distinct distributions (Figures 4K and 4L; Table S2). Boltzmann slopes and F_{50} values were normally distributed in telogen but followed log normal distributions in anagen. Catagen represented an intermediate phase, with parameters following normal distributions for dynamic firing, but not for static firing. These different distributions precluded direct comparison of variance between populations; however, anagen data displayed more pronounced rightward skew than telogen populations (Table S2). Overall, 29% of afferents in anagen and catagen displayed markedly lower sensitivities (Figure 4K) and high mechanical set-points compared with telogen afferents (Figures 4L and 4M). Together these data suggest that, in the midst of afferent remodeling, Merkel-cell afferents

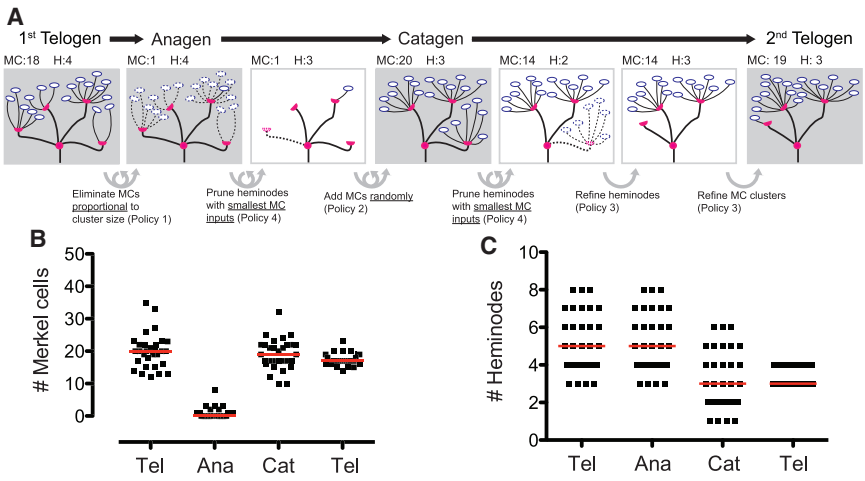

Figure 3. Computational Simulations Reveal Principles of End-Organ Remodeling

(A) Schematic of a simulation. Hair cycle stages and Merkel cell (MC) and heminode (H) counts are indicated above, and remodeling policies are summarized below. Blue ovals, Merkel cells; magenta half circles, heminodes; dashed lines, eliminated structures; looped arrows, iterative steps.

(B and C) Each square represents a single auto-generated afferent that progressed through simulation. Predicted distributions of Merkel cell numbers (B) and heminodes (C) at the indicated hair cycle stages. Red lines, medians.

are mechanosensitive but their ability to encode gentle touch is compromised.

We wondered whether these physiological differences might have behavioral consequences. In an attempt to evaluate the contribution of SA afferents in hairy skin, we modified a tape response assay (Bouet et al., 2009; Ranade et al., 2014) by applying a small sticker to the lower back after hair removal (Figures 5A and 5B). This paradigm delivers sustained pressure, whereas stroking or air puff represents a dynamic stimulus that engages rapidly adapting receptors (Bai et al., 2015; Garrison et al., 2012). Mice had fewer detections, defined as touching the sticker with either the nose or paw, in anagen (n = 109/117 trials in 20 mice) compared with telogen (n = 114/115 trials in 20 mice; p = 0.036, two-tailed Fisher's exact test). Moreover, detection latencies were significantly longer in anagen than in telogen (Figure 5C; p = 0.0014, Wilcoxon matched-pairs signed-rank test). Thus, we conclude that behavioral responsiveness to tactile pressure is reduced in anagen.

DISCUSSION

This study reveals the remarkable plasticity of the peripheral nervous system in healthy skin. Our results demonstrate that Merkel-cell afferents are capable of dramatic remodeling over a few days. Although the turnover of sensory epithelia is established in taste buds and the olfactory system, the mechanisms that preserve proper innervation in these tissues are not well defined (Castillo et al., 2014; Ma et al., 2014; Tsai and Barnea, 2014). We found that the skin's nervous system undergoes renewal as a part of normal epithelial remodeling, which highlights the utility of the mouse hair cycle as a system for studying pathways that govern intrinsic neuronal remodeling programs in the absence of injury or pathophysiology.

Plasticity in Merkel-Cell Afferents

Structural analysis of tactile afferents demonstrated that both myelinated and unmyelinated branches remodel over the hair cycle. Interestingly, these two domains in the peripheral arbor follow different trajectories: unmyelinated neurites fluctuate in tandem with Merkel cell numbers, whereas myelinated branches refine progressively. Future studies are needed to determine whether common mechanisms govern these processes.

Computational simulations indicate that simple principles of plasticity can account for the distributions of Merkel cell and heminode numbers observed in the spontaneous hair cycle. In particular, the model suggests that Merkel cells are stochastically incorporated into the arbor but that heminodes with low Merkel-cell numbers are pruned. The correlation between Merkel-cell number and heminodes during catagen supports the validity of these principles, as end organs with more Merkel cells also have more heminodes. The reduction of Merkel cells during anagen coincided with the loss of neurites in touch-dome afferents, raising the possibility that these cell types are inter-dependent. It is unlikely that loss of Merkel cells drives neuronal remodeling, as touch-dome innervation does not require intact Merkel cells (Maricich et al., 2009; Reed-Geaghan et al., 2016). By contrast, intact innervation and neurally-derived signals are needed to maintain full complements of touch-dome Merkel cells (Nurse et al., 1984; Xiao et al., 2015). Our observation that innervation and Merkel cells change in concert over a few days extend this model by suggesting a tight temporal dependence of touch-dome Merkel cells on intact innervation. Note, however, that the Merkel cell's neural dependency differs across tissues (Mills et al., 1989; Ebara et al., 2002).

Lineage-tracing studies report that Merkel cells are replenished slowly from epidermal progenitors, with a lifespan of at least 7 weeks (Doucet et al., 2013; Wright et al., 2015). Nonetheless, most Merkel cells are newly specified over the course of two hair cycles (Xiao et al., 2015). Our observation that touch domes had few Merkel cells in late anagen but normal Merkel-cell complements in catagen indicates that Merkel cells might undergo rapid turnover. Alternatively, it is possible that Merkel cells are not replaced but display coordinated changes in Merkel-specific protein expression over the hair cycle. Additional studies are needed to distinguish between these mechanisms.

Our finding that Merkel-cell numbers transiently decrease in anagen contrasts with previous reports that keratin 20 (K20)-positive Merkel cells in back skin are most abundant in anagen (Moll et al., 1996; Nakafusa et al., 2006). This apparent discrepancy is unlikely to be caused by the use of different Merkel-cell markers, because K20 and K8 co-localize in 99% of mouse Merkel cells (Wright et al., 2015). Moreover, we confirmed the loss of

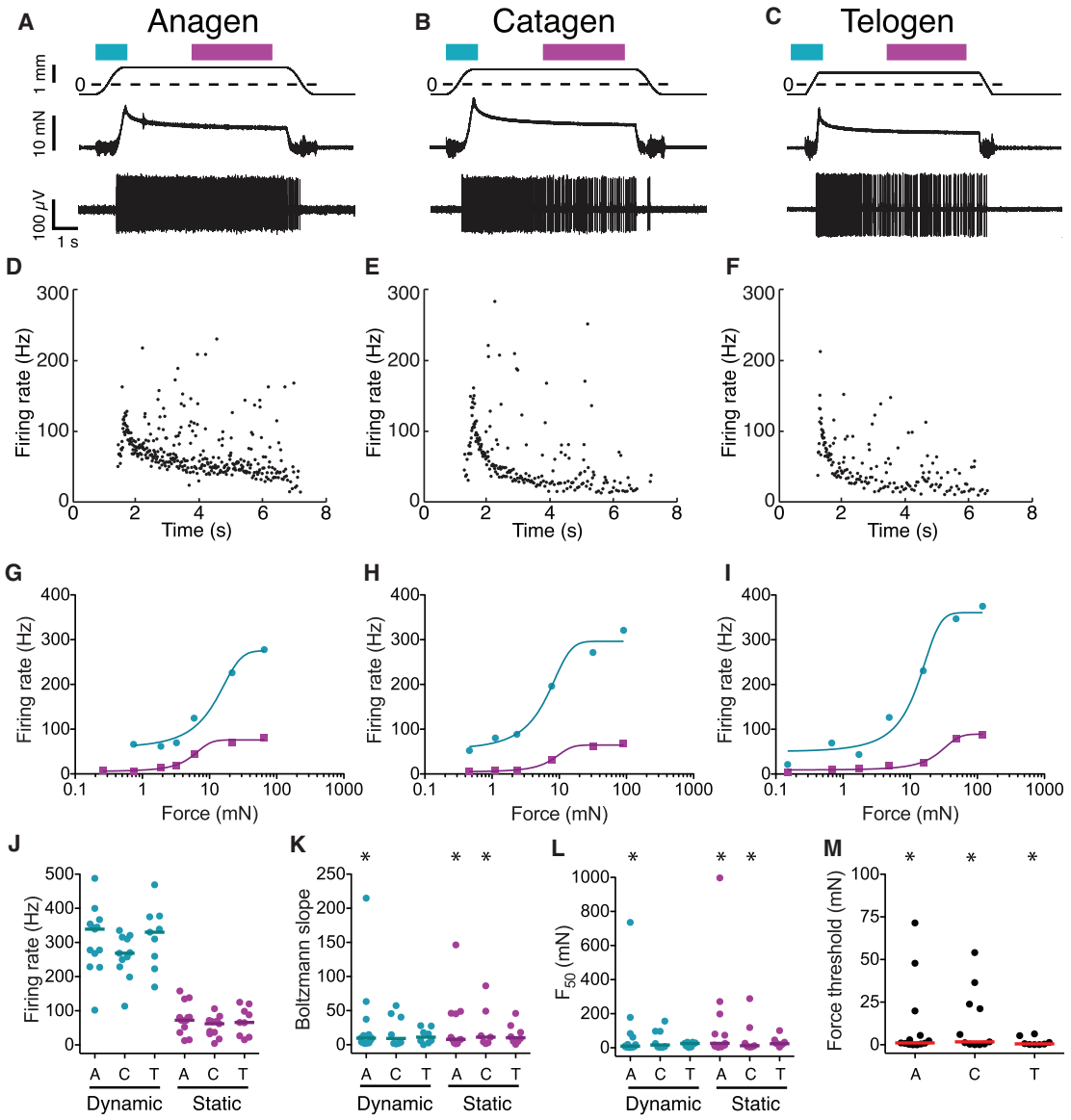

Figure 4. SAI Response Properties Are Less Reliable during the Hair Cycle

(A–C) Representative traces show SAI responses in spontaneous anagen (A), catagen (B), and telogen (C). Top traces show displacements, with dashed 0 lines indicating point of probe contact with skin. Bars denote stimulus phases (teal, dynamic; magenta, static). Middle traces show forces. Lower traces show action potential trains.

(D–F) Instantaneous firing frequency versus time for the traces above is shown.

(G–I) Stimulus-response curves of the units in (A)–(C).

(J–M) Aggregate data in anagen (A; n = 13 units), catagen (C; n = 11 units), and telogen (T; n = 9 units). Maximal firing rates (J), Boltzmann slopes (K), mid-points of Boltzmann fits (F_{50}) (L), and force thresholds (M) are shown. Asterisks mark non-normal distributions ($p \leq 0.05$, Kolmogorov-Smirnov test). Lines, medians. See also Table S2.

Merkel-cell-specific protein expression with two additional markers. Other methodological differences might account for this disparity. First, a study of plucking-induced hair cycles quantified Merkel cells in histological sections, which inherently undersamples rare cell types (Moll et al., 1996). Second, an analysis of Merkel-cell numbers in rat back skin by whole-mount immunohistochemistry found that dendritic Merkel cells peak in mid-anagen and progressively decrease through late anagen (Nakafusa et al., 2006). This progressive decrease is consistent with our observations in the mouse; however, the peak in Merkel cells in mid-anagen might reflect a species difference.

The surprising degree of afferent plasticity during hair growth raises the question of whether hair cycle-stimulated remodeling is required for afferent maintenance. Interestingly, *Hairless* mice, whose follicles do not cycle, have innervated Merkel cells, indicating that the hair cycle itself is not needed to maintain

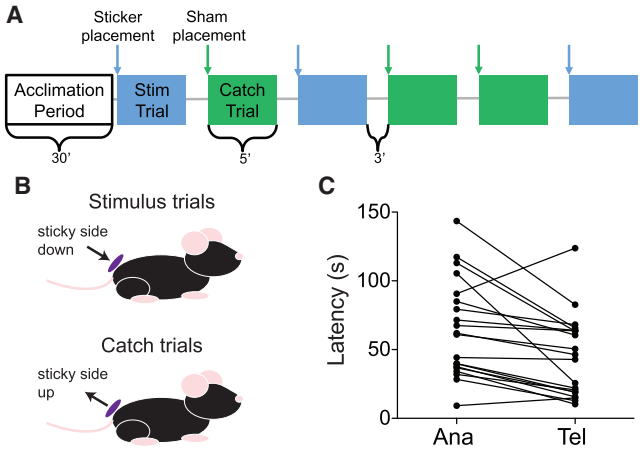

Figure 5. Behavioral Touch Responses Are Impaired during Anagen

(A) Behavioral testing paradigm. The order of stimulus (blue) and catch trials (green) was randomized.

(B) Diagram shows sticker placement.

(C) Latency to sticker detection at each hair cycle stage. Dots represent the mean latency for three to six trials per mouse. Lines connect latencies from individual mice ($p = 0.001$, Wilcoxon matched-pairs signed-rank test).

Merkel-cell end organs (Xiao et al., 2015). Thus, we propose that neuronal plasticity is a normal process that is synchronized by hair growth.

Functional Consequences of Afferent Plasticity

Electrophysiological recordings demonstrated that touch reception is maintained during anagen and catagen but that mechanical sensitivity is compromised in many afferents during these stages. Such changes might reflect differences in terminal architecture or alterations in ion channels that govern neuronal excitability. Changes in skin geometry also might alter tactile sensitivity; however, the impact of tissue properties can be minimized if neurons encode compressive stress rather than strain (Wang et al., 2016; Ge and Khalsa, 2002). Given that most touch-dome afferents produced typical SAI responses, it is also possible that tactile sensitivity is largely preserved through homeostatic changes in excitability that offset differences in end-organ structure and skin geometry.

Because recent studies have shown that touch dome afferents that lack mechanosensitive Merkel cells produce intermediately adapting (IA) firing patterns (Maksimovic et al., 2014; Woo et al., 2014), we expected to observe IA responses in late anagen. Instead, almost all touch dome units had SA firing patterns. We speculate that these responses are produced by intact Merkel-cell afferents. Alternatively, touch dome afferents might produce sustained firing when Merkel cells are lost post-natally (Kinkelin et al., 1999). We favor the former model because optogenetic silencing of Merkel cells attenuates sustained SAI firing (Baumbauer et al., 2015; Maksimovic et al., 2014), which demonstrates that Merkel-cell activity is required.

Our behavioral studies show that mice in anagen have impaired tactile responsiveness to sustained pressure. Future studies will delineate whether morphological and functional changes extend to other afferent subtypes. This surprising result also suggests that, evolutionarily, the benefits of afferent remodeling offset a transient loss in tactile sensitivity.

Hair-Cycle-Signaling Pathways

Molecular signals from follicular and dermal cells could be driving the hair cycle-associated changes observed in neurons and Merkel cells. Several pathways that are required for hair cycling also are involved in neuronal outgrowth and Merkel-cell maintenance, including bone morphogenetic proteins (Plikus et al., 2008; Kobielak et al., 2007; Bhattacherjee et al., 2013), sonic hedgehog (Oro and Higgins, 2003; Xiao et al., 2015), and fibroblast growth factor 5 (Scarlato et al., 2001; Suzuki et al., 2000; Hébert et al., 1994). The results of this study set the stage for assessing the role of these hair cycle-signaling pathways in control of cutaneous innervation.

Somatosensory neurons undergo degeneration and sprouting after injury and in skin diseases (Kinkelin et al., 2000; Taneda et al., 2011). It is possible that mechanisms of healthy neuronal remodeling and pathological neurite clearance are shared. Axon remodeling in the context of injury is a multi-faceted, active process governed by cues from the soma (Barnett et al., 2016; Cashman and Höke, 2015; Gerdts et al., 2015). Moreover, neurotrophins are upregulated in skin during injury-induced neuronal sprouting (Constantinou et al., 1994; Jankowski and Koerber, 2010; Quarta et al., 2014). Maintenance programs could piggyback on these injury pathways. Delineating and harnessing these processes at a molecular level could allow for interventions to improve touch-receptor recovery after injury and maintenance of touch receptors during aging.

EXPERIMENTAL PROCEDURES

Detailed methods are included in the Supplemental Experimental Procedures. Statistical tests were selected based on number of groups to be compared and normality of data, and they are indicated in the text and figure legends.

Animal studies complied with the Institutional Animal Care and Use Committee of Columbia University. Specimens were collected from mice during either the first spontaneous hair cycle or a plucking-induced hair cycle. Hair-cycle stages were verified histologically as described (Müller-Röver et al., 2001). Late anagen was defined as anagen IV–VI. C57BL/6 mice were used except where indicated. Electrophysiology, quantitative immunohistochemistry, and 3D reconstructions were performed as previously described (Maksimovic et al., 2014; Lesniak et al., 2014).

Tactile sensitivity was tested using a modified version of the tape response test (Bouet et al., 2009; Ranade et al., 2014). Two cohorts ($n = 10$ mice each) were tested on their ability to detect a sticker placed on depilated skin in anagen and second telogen.

Computational simulations were programmed in Python. Transitions between hair cycle stages were modeled as separate simulations.

SUPPLEMENTAL INFORMATION

Supplemental Information includes Supplemental Experimental Procedures, four figures, two tables, and four movies and can be found with this article online at http://dx.doi.org/10.1016/j.celrep.2016.10.034.

AUTHOR CONTRIBUTIONS

Conceptualization, K.L.M., G.J.G., and E.A.L.; Software, R.L.O. and G.J.G.; Validation, R.C.C.; Formal Analysis, K.L.M., R.C.C., Y.B., R.L.O., G.J.G., and E.A.L.; Investigation, K.L.M., R.C.C., and Y.B.; Writing – Original Draft, K.L.M. and R.C.C.; Writing – Review & Editing, K.L.M., R.C.C., Y.B., R.L.O.,

G.J.G., and E.A.L.; Visualization, K.L.M., R.C.C., and E.A.L.; Supervision, E.A.L.; Project Administration, E.A.L.; Funding Acquisition, G.J.G. and E.A.L.

ACKNOWLEDGMENTS

We thank Dr. Seung Woo for assistance with *Piezo2-gfp* mice, Ms. Emily Chang for help with hair-cycle induction, and Ms. Milda Stanislauskas for histology. Ms. Blair Jenkins contributed to early project stages. Drs. David Owens, Angela Christiano, and Diana Bautista and members of the E.A.L., G.J.G., and Angela Christiano laboratories provided helpful discussions. This research was supported by NINDS R01NS073119 (to E.A.L. and G.J.G.). R.C.C. was supported by NICHD 2T32HD007430-18 and NINDS 5T32NS064928-07. Core facilities were supported by the Columbia University EpiCURE Center (NIAMS P30AR069632) and the Herbert Irving Comprehensive Cancer Center (NCI P30CA013696).

Received: June 1, 2016
Revised: September 21, 2016
Accepted: October 12, 2016
Published: November 8, 2016

REFERENCES

Alonso, L., and Fuchs, E. (2006). The hair cycle. J. Cell Sci. *119*, 391–393.

Bai, L., Lehnert, B.P., Liu, J., Neubarth, N.L., Dickendesher, T.L., Nwe, P.H., Cassidy, C., Woodbury, C.J., and Ginty, D.D. (2015). Genetic identification of an expansive mechanoreceptor sensitive to skin stroking. Cell *163*, 1783–1795.

Barnett, M.H., Mathey, E., Kiernan, M.C., and Pollard, J.D. (2016). Axonal damage in central and peripheral nervous system inflammatory demyelinating diseases: common and divergent pathways of tissue damage. Curr. Opin. Neurol. *29*, 213–221.

Baumbauer, K.M., DeBerry, J.J., Adelman, P.C., Miller, R.H., Hachisuka, J., Lee, K.H., Ross, S.E., Koerber, H.R., Davis, B.M., and Albers, K.M. (2015). Keratinocytes can modulate and directly initiate nociceptive responses. eLife *4*, e09674.

Bhattacherjee, A., Rumi, M.A., Staecker, H., and Smith, P.G. (2013). Bone morphogenetic protein 4 mediates estrogen-regulated sensory axon plasticity in the adult female reproductive tract. J. Neurosci. *33*, 1050–61a.

Botchkarev, V.A., Eichmüller, S., Johansson, O., and Paus, R. (1997). Hair cycle-dependent plasticity of skin and hair follicle innervation in normal murine skin. J. Comp. Neurol. *386*, 379–395.

Bouet, V., Boulouard, M., Toutain, J., Divoux, D., Bernaudin, M., Schumann-Bard, P., and Freret, T. (2009). The adhesive removal test: a sensitive method to assess sensorimotor deficits in mice. Nat. Protoc. *4*, 1560–1564.

Cashman, C.R., and Höke, A. (2015). Mechanisms of distal axonal degeneration in peripheral neuropathies. Neurosci. Lett. *596*, 33–50.

Castillo, D., Seidel, K., Salcedo, E., Ahn, C., de Sauvage, F.J., Klein, O.D., and Barlow, L.A. (2014). Induction of ectopic taste buds by SHH reveals the competency and plasticity of adult lingual epithelium. Development *141*, 2993–3002.

Chen, Z.L., Yu, W.M., and Strickland, S. (2007). Peripheral regeneration. Annu. Rev. Neurosci. *30*, 209–233.

Cheng, C., Guo, G.F., Martinez, J.A., Singh, V., and Zochodne, D.W. (2010). Dynamic plasticity of axons within a cutaneous milieu. J. Neurosci. *30*, 14735–14744.

Constantinou, J., Reynolds, M.L., Woolf, C.J., Safieh-Garabedian, B., and Fitzgerald, M. (1994). Nerve growth factor levels in developing rat skin: upregulation following skin wounding. Neuroreport *5*, 2281–2284.

Doucet, Y.S., Woo, S.H., Ruiz, M.E., and Owens, D.M. (2013). The touch dome defines an epidermal niche specialized for mechanosensory signaling. Cell Rep. *3*, 1759–1765.

Dubový, P., and Aldskogius, H. (1996). Degeneration and regeneration of cutaneous sensory nerve formations. Microsc. Res. Tech. *34*, 362–375.

Ebara, S., Kumamoto, K., Matsuura, T., Mazurkiewicz, J.E., and Rice, F.L. (2002). Similarities and differences in the innervation of mystacial vibrissal follicle-sinus complexes in the rat and cat: a confocal microscopic study. J. Comp. Neurol. *449*, 103–119.

Feng, P., Huang, L., and Wang, H. (2014). Taste bud homeostasis in health, disease, and aging. Chem. Senses *39*, 3–16.

Fuchs, E. (2009). The tortoise and the hair: slow-cycling cells in the stem cell race. Cell *137*, 811–819.

Garrison, S.R., Dietrich, A., and Stucky, C.L. (2012). TRPC1 contributes to light-touch sensation and mechanical responses in low-threshold cutaneous sensory neurons. J. Neurophysiol. *107*, 913–922.

Ge, W., and Khalsa, P.S. (2002). Encoding of compressive stress during indentation by slowly adapting type I mechanoreceptors in rat hairy skin. J. Neurophysiol. *87*, 1686–1693.

Gerdts, J., Brace, E.J., Sasaki, Y., DiAntonio, A., and Milbrandt, J. (2015). SARM1 activation triggers axon degeneration locally via NAD^+ destruction. Science *348*, 453–457.

Haeberle, H., Fujiwara, M., Chuang, J., Medina, M.M., Panditrao, M.V., Bechstedt, S., Howard, J., and Lumpkin, E.A. (2004). Molecular profiling reveals synaptic release machinery in Merkel cells. Proc. Natl. Acad. Sci. USA *101*, 14503–14508.

Hébert, J.M., Rosenquist, T., Götz, J., and Martin, G.R. (1994). FGF5 as a regulator of the hair growth cycle: evidence from targeted and spontaneous mutations. Cell *78*, 1017–1025.

Hsieh, S.T., Chiang, H.Y., and Lin, W.M. (2000). Pathology of nerve terminal degeneration in the skin. J. Neuropathol. Exp. Neurol. *59*, 297–307.

Iggo, A., and Muir, A.R. (1969). The structure and function of a slowly adapting touch corpuscle in hairy skin. J. Physiol. *200*, 763–796.

Jahoda, C.A., and Christiano, A.M. (2011). Niche crosstalk: intercellular signals at the hair follicle. Cell *146*, 678–681.

Jankowski, M.P., and Koerber, H.R. (2010). Neurotrophic factors and nociceptor sensitization. In Translational Pain Research: From Mouse to Man, L. Kruger and A.R. Light, eds. (Boca Raton, FL: CRC Press).

Johnson, K.O., Yoshioka, T., and Vega-Bermudez, F. (2000). Tactile functions of mechanoreceptive afferents innervating the hand. J. Clin. Neurophysiol. *17*, 539–558.

Kim, D.K., and Holbrook, K.A. (1995). The appearance, density, and distribution of Merkel cells in human embryonic and fetal skin: their relation to sweat gland and hair follicle development. J. Invest. Dermatol. *104*, 411–416.

Kinkelin, I., Stucky, C.L., and Koltzenburg, M. (1999). Postnatal loss of Merkel cells, but not of slowly adapting mechanoreceptors in mice lacking the neurotrophin receptor p75. Eur. J. Neurosci. *11*, 3963–3969.

Kinkelin, I., Mötzing, S., Koltenzenburg, M., and Bröcker, E.B. (2000). Increase in NGF content and nerve fiber sprouting in human allergic contact eczema. Cell Tissue Res. *302*, 31–37.

Kobielak, K., Stokes, N., de la Cruz, J., Polak, L., and Fuchs, E. (2007). Loss of a quiescent niche but not follicle stem cells in the absence of bone morphogenetic protein signaling. Proc. Natl. Acad. Sci. USA *104*, 10063–10068.

Lesniak, D.R., Marshall, K.L., Wellnitz, S.A., Jenkins, B.A., Baba, Y., Rasband, M.N., Gerling, G.J., and Lumpkin, E.A. (2014). Computation identifies structural features that govern neuronal firing properties in slowly adapting touch receptors. eLife *3*, e01488.

Li, L., Rutlin, M., Abraira, V.E., Cassidy, C., Kus, L., Gong, S., Jankowski, M.P., Luo, W., Heintz, N., Koerber, H.R., et al. (2011). The functional organization of cutaneous low-threshold mechanosensory neurons. Cell *147*, 1615–1627.

Ma, L., Wu, Y., Qiu, Q., Scheerer, H., Moran, A., and Yu, C.R. (2014). A developmental switch of axon targeting in the continuously regenerating mouse olfactory system. Science *344*, 194–197.

Maksimovic, S., Nakatani, M., Baba, Y., Nelson, A.M., Marshall, K.L., Wellnitz, S.A., Firozi, P., Woo, S.H., Ranade, S., Patapoutian, A., and Lumpkin, E.A. (2014). Epidermal Merkel cells are mechanosensory cells that tune mammalian touch receptors. Nature *509*, 617–621.

Maricich, S.M., Wellnitz, S.A., Nelson, A.M., Lesniak, D.R., Gerling, G.J., Lumpkin, E.A., and Zoghbi, H.Y. (2009). Merkel cells are essential for light-touch responses. Science *324*, 1580–1582.

Mills, L.R., Nurse, C.A., and Diamond, J. (1989). The neural dependency of Merkel cell development in the rat: the touch domes and foot pads contrasted. Dev. Biol. *136*, 61–74.

Moll, I., Paus, R., and Moll, R. (1996). Merkel cells in mouse skin: intermediate filament pattern, localization, and hair cycle-dependent density. J. Invest. Dermatol. *106*, 281–286.

Mouret, A., Lepousez, G., Gras, J., Gabellec, M.M., and Lledo, P.M. (2009). Turnover of newborn olfactory bulb neurons optimizes olfaction. J. Neurosci. *29*, 12302–12314.

Müller-Röver, S., Handjiski, B., van der Veen, C., Eichmüller, S., Foitzik, K., McKay, I.A., Stenn, K.S., and Paus, R. (2001). A comprehensive guide for the accurate classification of murine hair follicles in distinct hair cycle stages. J. Invest. Dermatol. *117*, 3–15.

Nakafusa, J., Narisawa, Y., Shinogi, T., Taira, K., Tanaka, T., Inoue, T., and Misago, N. (2006). Changes in the number of Merkel cells with the hair cycle in hair discs on rat back skin. Br. J. Dermatol. *155*, 883–889.

Nurse, C.A., Macintyre, L., and Diamond, J. (1984). Reinnervation of the rat touch dome restores the Merkel cell population reduced after denervation. Neuroscience *13*, 563–571.

Oro, A.E., and Higgins, K. (2003). Hair cycle regulation of Hedgehog signal reception. Dev. Biol. *255*, 238–248.

Peters, E.M., Botchkarev, V.A., Botchkareva, N.V., Tobin, D.J., and Paus, R. (2001). Hair-cycle-associated remodeling of the peptidergic innervation of murine skin, and hair growth modulation by neuropeptides. J. Invest. Dermatol. *116*, 236–245.

Plikus, M.V., and Chuong, C.M. (2008). Complex hair cycle domain patterns and regenerative hair waves in living rodents. J. Invest. Dermatol. *128*, 1071–1080.

Plikus, M.V., Mayer, J.A., de la Cruz, D., Baker, R.E., Maini, P.K., Maxson, R., and Chuong, C.M. (2008). Cyclic dermal BMP signalling regulates stem cell activation during hair regeneration. Nature *451*, 340–344.

Quarta, S., Baeumer, B.E., Scherbakov, N., Andratsch, M., Rose-John, S., Dechant, G., Bandtlow, C.E., and Kress, M. (2014). Peripheral nerve regeneration and NGF-dependent neurite outgrowth of adult sensory neurons converge on STAT3 phosphorylation downstream of neuropoietic cytokine receptor gp130. J. Neurosci. *34*, 13222–13233.

Rajan, B., Polydefkis, M., Hauer, P., Griffin, J.W., and McArthur, J.C. (2003). Epidermal reinnervation after intracutaneous axotomy in man. J. Comp. Neurol. *457*, 24–36.

Ranade, S.S., Woo, S.H., Dubin, A.E., Moshourab, R.A., Wetzel, C., Petrus, M., Mathur, J., Bégay, V., Coste, B., Mainquist, J., et al. (2014). Piezo2 is the major transducer of mechanical forces for touch sensation in mice. Nature *516*, 121–125.

Reed-Geaghan, E.G., Wright, M.C., See, L.A., Adelman, P.C., Lee, K.H., Koerber, H.R., and Maricich, S.M. (2016). Merkel cell-driven BDNF signaling specifies SAI neuron molecular and electrophysiological phenotypes. J. Neurosci. *36*, 4362–4376.

Scarlato, M., Xu, T., Bannerman, P., Beesley, J., Reddy, U.R., Rostami, A., Scherer, S.S., and Pleasure, D. (2001). Axon-Schwann cell interactions regulate the expression of fibroblast growth factor-5 (FGF-5). J. Neurosci. Res. *66*, 16–22.

Schneider, M.R., Schmidt-Ullrich, R., and Paus, R. (2009). The hair follicle as a dynamic miniorgan. Curr. Biol. *19*, R132–R142.

Suzuki, S., Ota, Y., Ozawa, K., and Imamura, T. (2000). Dual-mode regulation of hair growth cycle by two Fgf-5 gene products. J. Invest. Dermatol. *114*, 456–463.

Taneda, K., Tominaga, M., Negi, O., Tengara, S., Kamo, A., Ogawa, H., and Takamori, K. (2011). Evaluation of epidermal nerve density and opioid receptor levels in psoriatic itch. Br. J. Dermatol. *165*, 277–284.

Tsai, L., and Barnea, G. (2014). A critical period defined by axon-targeting mechanisms in the murine olfactory bulb. Science *344*, 197–200.

Wang, Y., Baba, Y., Lumpkin, E.A., and Gerling, G.J. (2016). Computational modeling indicates that surface pressure can be reliably conveyed to tactile receptors even amidst changes in skin mechanics. J. Neurophysiol. *116*, 218–228.

Wellnitz, S.A., Lesniak, D.R., Gerling, G.J., and Lumpkin, E.A. (2010). The regularity of sustained firing reveals two populations of slowly adapting touch receptors in mouse hairy skin. J. Neurophysiol. *103*, 3378–3388.

Woo, S.H., Ranade, S., Weyer, A.D., Dubin, A.E., Baba, Y., Qiu, Z., Petrus, M., Miyamoto, T., Reddy, K., Lumpkin, E.A., et al. (2014). Piezo2 is required for Merkel-cell mechanotransduction. Nature *509*, 622–626.

Wright, M.C., Reed-Geaghan, E.G., Bolock, A.M., Fujiyama, T., Hoshino, M., and Maricich, S.M. (2015). Unipotent, Atoh1+ progenitors maintain the Merkel cell population in embryonic and adult mice. J. Cell Biol. *208*, 367–379.

Xiao, Y., Thoresen, D.T., Williams, J.S., Wang, C., Perna, J., Petrova, R., and Brownell, I. (2015). Neural Hedgehog signaling maintains stem cell renewal in the sensory touch dome epithelium. Proc. Natl. Acad. Sci. USA *112*, 7195–7200.